

A Predictive Non-Holomorphic Modular A_4 Linear Seesaw Framework Testable at DUNE

Rudra Majhi,^a Mitesh Kumar Behera^b Rukmani Mohanta^c

^a*Department of Physics, Nabarangpur College, Nabarangpur, Odisha, 764059, India*

^b*Department of Physics, School of Advanced Sciences, Vellore Institute of Technology, Tiruvallam Rd, Katpadi, Vellore, Tamil Nadu 632014, India*

^c*School of Physics, University of Hyderabad, Hyderabad-500046, India*

E-mail: rudra.majhi95@gmail.com, miteshbehera1304@gmail.com,
rmsp@uohyd.ac.in

ABSTRACT: We study a realization of neutrino masses within the linear seesaw mechanism based on non-holomorphic modular A_4 symmetry, extending modular-invariant flavor models beyond the conventional holomorphic framework. The model is constructed in a non-supersymmetric setting and involves six heavy $SU(2)_L$ singlet fermions, N_R and S_L , together with a single flavon field, thereby significantly reducing the field content. The modular transformation properties of the Yukawa couplings under A_4 symmetry lead to a highly constrained neutrino mass matrix with a distinctive flavor structure. After presenting the general theoretical framework, we perform a systematic numerical analysis of neutrino phenomenology by restricting the modulus parameter τ to the fundamental domain and scanning the allowed parameter space. We identify regions consistent with current neutrino oscillation data at the 3σ level and obtain predictions for currently unknown observables, including the absolute neutrino mass scale and leptonic CP-violating phases. We further examine the implications for neutrinoless double beta decay, highlighting testable signatures in upcoming precision oscillation and rare-process experiments. These results demonstrate the phenomenological viability and predictive power of non-holomorphic modular symmetry in linear seesaw neutrino mass models.

Contents

1	Introduction	1
2	Non-Holomorphic Modular Symmetry	3
3	MODEL FRAMEWORK	4
3.1	Dirac mass term for charged leptons (M_ℓ)	5
3.2	Dirac and pseudo-Dirac mass terms	6
3.3	Mixing between the heavy fields N_R and S_L^c	7
3.4	Majorana term for N_R	7
3.5	Linear Seesaw mechanism for light neutrino masses	7
3.6	Neutrino Oscillation Observables	8
4	Simulation Details	9
5	Results	10
5.1	Predictions from the model	10
5.2	Neutrinoless Double Beta Decay	12
6	Summary and Conclusions	16
A	Modular Yukawa couplings	17
B	Block Diagonalization	18

1 Introduction

The Standard Model (SM) falls short in explaining the observed properties of neutrinos. While it predicts neutrinos to be massless, experimental results show that they have tiny but non-zero masses [1–4], as confirmed by neutrino oscillation data. Neutrino oscillations are now firmly established and provide strong evidence that neutrinos mix with each other, with at least two of them having non-zero masses [5]. In the SM, neutrinos lack right-handed (RH) counterparts, which prevents them from acquiring Dirac masses like other charged fermions. However, the dimension-five Weinberg operator [6–8] offers a way to generate neutrino masses. Still, the fundamental origin and flavor structure of this operator remain open questions.

Therefore, it becomes essential to explore scenarios beyond the Standard Model (BSM) to account for the non-zero masses of neutrinos. Several models have been proposed in the literature to explain the results from neutrino oscillation experiments. These include the well-known seesaw mechanism [9–11], radiative mass generation models [12, 13], and

frameworks involving extra dimensions [14], among others. A common feature of many such BSM approaches is the introduction of SM gauge singlet fermions, often identified as right-handed neutrinos, that couple to active neutrinos via Yukawa interactions. Their masses and couplings can vary across many orders of magnitude, leading to a wide range of possible phenomenological implications. For instance, in the canonical seesaw mechanism, explaining eV-scale light neutrino masses typically requires right-handed neutrino masses around 10^{15} GeV, which is far beyond the reach of present or future experiments. In contrast, low-scale variants such as the inverse seesaw [15–17], linear seesaw [18], and extended seesaw [19] allow the heavy neutrinos to lie at the TeV scale, making them accessible to experimental verification.

The non-Abelian discrete flavor symmetry group A_4 has long been considered a compelling framework for explaining the structure of the neutrino mass matrix [20, 21]. In its simplest realization, however, it predicts a vanishing reactor mixing angle θ_{13} , which contradicts experimental observations. To reconcile this, additional flavon fields, Standard Model singlet scalars transforming non-trivially under A_4 are typically introduced. Their vacuum alignments break the flavor symmetry spontaneously, generating a non-zero θ_{13} and reproducing realistic mixing patterns [22]. Despite these successes, such constructions often rely on multiple flavons and higher-dimensional operators, which can obscure predictability and restrict the flavor symmetry’s role to constraining mixing angles rather than determining the full neutrino mass structure.

A more predictive and elegant alternative arises in the *modular invariance approach* originally proposed by [23] and thereafter followed by myriad literature [24–49]. Here, Yukawa couplings are promoted to *modular forms*, transforming under the finite modular groups $\Gamma(N)$ or $\Gamma'(N)$. This framework naturally eliminates the need for flavon fields while maintaining a high degree of theoretical control. Traditionally studied in supersymmetric (SUSY) settings, modular symmetry ensures holomorphicity of the superpotential. However, with the absence of low-energy SUSY signals and growing experimental constraints, recent developments have extended this idea to *non-holomorphic modular symmetries* originally given by [50], vastly enriching the theoretical landscape.

In particular, *polyharmonic Maaß modular forms*, which contain both holomorphic and non-holomorphic components, provide a broader and more flexible structure for model building. These forms satisfy Laplacian conditions and decompose into irreducible representations of $\Gamma(N)$ or $\Gamma'(N)$, allowing for richer flavor dynamics without invoking additional scalar fields. This expanded framework offers distinct advantages: it maintains modular predictability, accommodates radiative and non-super-symmetric effects, and provides new avenues for generating viable neutrino masses and mixings as shown in Refs.[51–72]. Thus, non-holomorphic modular invariance not only overcomes the limitations of discrete flavor models but also establishes a versatile and predictive framework for neutrino physics that does not involve super-symmetry.

The structure of this paper is as follows. In Sec. 2, we outline the brief insights into non-holomorphic modular symmetry. We then provide a discussion of the light neutrino masses and mixing in this model framework in Sec. 3, and simulation details are discussed

in Sec. 4. Further in Sec. 5, a numerical correlational study is established between observables of the neutrino sector and model input parameters. In Section 6, we conclude our results.

2 Non-Holomorphic Modular Symmetry

Modular symmetry arises geometrically as the symmetry of a two-dimensional torus. A torus T^2 is constructed by identifying points in the Euclidean plane \mathbb{R}^2 under translations of a lattice Λ , such that $T^2 = \mathbb{R}^2/\Lambda$. In the complex representation, the lattice is spanned by two basis vectors, and the ratio of these vectors determines the complex structure of the torus [73, 74]. This ratio is encoded in the complex modulus $\tau = x + iy$, which transforms under modular symmetry as

$$\tau \longrightarrow \gamma\tau = \frac{a\tau + b}{c\tau + d}, \quad \gamma = \begin{pmatrix} a & b \\ c & d \end{pmatrix}, \quad (2.1)$$

where $a, b, c, d \in \mathbb{Z}$ satisfy $ad - bc = 1$. These transformations generate the modular group $SL(2, \mathbb{Z})$, representing the symmetry of the torus. Its finite quotients Γ_N for $N = 2, 3, 4, 5$ are isomorphic to the discrete groups S_3 [75–81], A_4 [82–94], S_4 [95–97], and A_5 [98, 99], respectively.

Modular invariance offers a predictive approach to flavor model building, providing an elegant explanation of fermion mass hierarchies and mixing structures. In $\mathcal{N} = 1$ super-symmetric (SUSY) constructions, modular symmetry has been successfully implemented to reproduce realistic lepton masses and mixing patterns with a minimal set of free parameters [23]. In such setups, matter superfields transform under representations of $SL(2, \mathbb{Z})$ (or its projective counterpart $PSL(2, \mathbb{Z})$), and the Yukawa couplings emerge as holomorphic modular forms of the modulus τ , defined over the upper half-plane.

While SUSY frameworks naturally ensure holomorphic Yukawa couplings, strong constraints from flavor observables, electroweak precision measurements, and astrophysical data severely limit the viable SUSY parameter space. Moreover, the absence of experimental evidence for low-energy super-symmetry motivates the exploration of non-SUSY realizations of modular flavor symmetry. It has been emphasized that the modular-form structure of Yukawa couplings is not intrinsically tied to super-symmetry; rather, it depends on the details of the compactification geometry. Recently, non-SUSY implementations of modular flavor symmetry have been developed using automorphic forms, where the holomorphicity condition is replaced by a Laplacian constraint. For a single complex modulus, these automorphic functions correspond to *harmonic Maaß forms*, which are non-holomorphic modular functions satisfying the Laplace equation. Consequently, modular flavor symmetry can be consistently realized even in the absence of SUSY [50].

Within this approach, the relevant mathematical objects are *polyharmonic Maaß forms* associated with the modulus τ . For a fixed level N , the finite modular group Γ'_N (or equivalently Γ_N) coincides with that of the holomorphic case. Generic matter fields ψ_i

and ψ_i^c transform under the modular symmetry with modular weights $-k_\psi$ and $-k_{\psi^c}$, and according to irreducible representations ρ_ψ and ρ_{ψ^c} of Γ'_N (or Γ_N), respectively:

$$\tau \rightarrow \gamma\tau = \frac{a\tau + b}{c\tau + d}, \quad \gamma = \begin{pmatrix} a & b \\ c & d \end{pmatrix} \in SL(2, \mathbb{Z}), \quad (2.2)$$

$$\psi_i(x) \rightarrow (c\tau + d)^{-k_\psi} [\rho_\psi(\gamma)]_{ij} \psi_j(x), \quad \psi_i^c(x) \rightarrow (c\tau + d)^{-k_{\psi^c}} [\rho_{\psi^c}(\gamma)]_{ij} \psi_j^c(x). \quad (2.3)$$

Fermion masses arise from Yukawa interactions of Dirac fermions. The modular-invariant Yukawa Lagrangian takes the form

$$\mathcal{L}_Y = Y^{(k_Y)}(\tau) \psi^c \psi H + \text{h.c.}, \quad (2.4)$$

where H denotes the Higgs field (or its conjugate) and fermion fields are written in two-component notation. Under modular transformations, the Higgs field transforms as

$$H(x) \rightarrow (c\tau + d)^{-k_H} \rho_H(\gamma) H(x). \quad (2.5)$$

The Yukawa couplings $Y^{(k_Y)}(\tau)$ are polyharmonic Maaß forms of weight k_Y at level N , transforming as

$$Y^{(k_Y)}(\gamma\tau) = (c\tau + d)^{k_Y} Y^{(k_Y)}(\tau), \quad \gamma = \begin{pmatrix} a & b \\ c & d \end{pmatrix} \in \Gamma(N), \quad (2.6)$$

and satisfying the Laplace equation and growth conditions:

$$-4y^2 \frac{\partial}{\partial \tau} \frac{\partial}{\partial \bar{\tau}} Y^{(k_Y)} + 2ik_Y y \frac{\partial}{\partial \bar{\tau}} Y^{(k_Y)} = 0, \quad Y^{(k_Y)}(\tau) = O(y^\alpha) \text{ as } y \rightarrow +\infty. \quad (2.7)$$

Modular invariance of the Yukawa interaction requires that the total modular weight vanishes and that the product of representations contains a singlet:

$$k_Y = k_{\psi^c} + k_\psi + k_H, \quad \rho_Y \otimes \rho_{\psi^c} \otimes \rho_\psi \otimes \rho_H \supset 1. \quad (2.8)$$

For Majorana fermions ψ^c , the corresponding mass term is written as

$$L_M = Y^{(k_Y)}(\tau) \psi^c \psi^c + \text{h.c.}, \quad (2.9)$$

with modular invariance conditions

$$k_Y = 2k_{\psi^c}, \quad \rho_Y \otimes \rho_{\psi^c} \otimes \rho_{\psi^c} \supset 1. \quad (2.10)$$

3 MODEL FRAMEWORK

This model represents the simplistic scenario of a linear seesaw, where the particle content and group charges are provided in Table 2. We prefer to extend with a discrete A_4 modular non-holomorphic symmetry to explore the neutrino phenomenology. The particle spectrum is enriched with six extra singlet heavy fermion fields (N_{Ri} and S_{Li}) and one flavon field

Weight k_Y	Polyharmonic Maaß forms $Y_r^{(k_Y)}$	
$k_Y = -2$	$Y_1^{(-2)}$,	$Y_3^{(-2)}$
$k_Y = 0$	$Y_1^{(0)}$,	$Y_3^{(0)}$

Table 1. Polyharmonic Maaß forms of weight $k_Y = -2, 0$ at level $N = 3$. The subscript r denotes the transformation property under A_4 modular symmetry.

(ϕ). The BSM fields of the model transform as a triplet under the A_4 modular symmetry group. Modular symmetry is broken when the complex modulus τ acquires a VEV $\langle \tau \rangle$ in the fundamental domain, fixing numerical values of modular forms $Y_r^{(k)}(\langle \tau \rangle)$ that determine flavor structures. The extra singlet flavon field is a trivial singlet under A_4 symmetry. The modular weight is assigned to all the particles and denoted as k_I , where the choice of modular weight is half integrals in order to avoid certain unwanted terms in the Lagrangian [66, 100]. The importance of A_4 modular symmetry is the requirement of fewer flavon fields, unlike the usual A_4 group, since the Yukawa couplings have the non-trivial group transformation. Assignment of group charge and modular weight to the Yukawa coupling is provided in Table 2.

Fields	L_e	L_μ	L_τ	e_R	μ_R	τ_R	N_R	S_L	H	ϕ
$SU(2)_L$	2	2	2	1	1	1	1	1	2	1
$U(1)_Y$	$-\frac{1}{2}$	$-\frac{1}{2}$	$-\frac{1}{2}$	-1	-1	-1	0	0	$\frac{1}{2}$	0
A_4	1	1'	1''	1	1'	1''	3	3	1	1
k_I	0	0	0	0	0	0	0	$-\frac{5}{2}$	0	$\frac{1}{2}$

Table 2. Field content and their transformation under $SU(2)_L \times U(1)_Y \times A_4$, and modular weights k_I .

3.1 Dirac mass term for charged leptons (M_ℓ)

To have a simplified structure for charged leptons mass matrix, we consider the three generations of left-handed doublets (L_e, L_μ, L_τ) transform as **1'**, **1''**, **1'** respectively under the A_4 symmetry. The right-handed charged leptons follow a transformation of **1**, **1'**, **1''** under A_4 symmetry respectively. All of them are assigned a modular weight of zero. The relevant Lagrangian term for charged leptons is given by

$$\mathcal{L}_{M_\ell} = y_\ell^{ee} L_e^c H e_R + y_\ell^{\mu\mu} L_\mu^c H \mu_R + y_\ell^{\tau\tau} L_\tau^c H \tau_R. \quad (3.1)$$

The charged lepton mass matrix is found to be diagonal, and the couplings can be adjusted to achieve the observed charged lepton masses. The mass matrix takes the form

$$M_\ell = \begin{pmatrix} y_\ell^{ee} v_d / \sqrt{2} & 0 & 0 \\ 0 & y_\ell^{\mu\mu} v_d / \sqrt{2} & 0 \\ 0 & 0 & y_\ell^{\tau\tau} v_d / \sqrt{2} \end{pmatrix} = \begin{pmatrix} m_e & 0 & 0 \\ 0 & m_\mu & 0 \\ 0 & 0 & m_\tau \end{pmatrix}. \quad (3.2)$$

Here, m_e , m_μ , and m_τ are the observed charged lepton masses.

3.2 Dirac and pseudo-Dirac mass terms

Along with the transformation of lepton doublets mentioned previously, the right-handed field N_R transforms as a triplet under the A_4 modular group. Since, with these charge assignments we can not write the standard interaction term, we introduce the Polyharmonic Maaß forms couplings to transform non-trivially under the non-holomorphic A_4 modular group (triplets) having modular weight of $k_Y = 0$, as represented in Table 1. We use the modular forms of the coupling as $\mathbf{Y}_3^{(0)}(\tau) = (Y_{3,1}^{(0)}, Y_{3,2}^{(0)}, Y_{3,3}^{(0)})$, expressed in Eqn. A.1, A.2, and A.3 (Appendix A). Therefore, the invariant Dirac Lagrangian involving the active and right-handed fields can be written as

$$\mathcal{L}_D = \alpha_D L_e^c \tilde{H} (\mathbf{Y}_3^{(0)} N_R)_1 + \beta_D L_\mu^c \tilde{H} (\mathbf{Y}_3^{(0)} N_R)_{1'} + \gamma_D L_\tau^c \tilde{H} (\mathbf{Y}_3^{(0)} N_R)_{1''} + \text{h.c.}, \quad (3.3)$$

Here, the subscript for the operator $\mathbf{Y}_3^{(0)} N_R$ indicates A_4 representation constructed by the product and $\{\alpha_D, \beta_D, \gamma_D\}$ are free parameters with $\tilde{x} = \frac{x}{\alpha_D}$ (i.e. $x = \beta_D, \gamma_D$) and $\tilde{H} = i\sigma H^*$. Using $v_H/\sqrt{2}$, where v_H is the vacuum expectation value (VEV) of H , the resulting Dirac mass matrix is given by

$$M_D = \frac{v_H}{\sqrt{2}} \alpha_D \begin{bmatrix} 1 & 0 & 0 \\ 0 & \tilde{\beta}_D & 0 \\ 0 & 0 & \tilde{\gamma}_D \end{bmatrix} \begin{bmatrix} Y_{3,1}^{(0)} & Y_{3,3}^{(0)} & Y_{3,2}^{(0)} \\ Y_{3,2}^{(0)} & Y_{3,1}^{(0)} & Y_{3,3}^{(0)} \\ Y_{3,3}^{(0)} & Y_{3,2}^{(0)} & Y_{3,1}^{(0)} \end{bmatrix}_{LR}. \quad (3.4)$$

As we also have the extra sterile fields S_L , which transform analogously to N_R under A_4 modular symmetry, the pseudo-Dirac term for the light neutrinos is allowed, and the corresponding Lagrangian is given as

$$\mathcal{L}_{LS} = \left[\alpha_{LS} L_{e_L} \tilde{H} (\mathbf{Y}_3^{(-2)} S_L^c)_1 + \beta_{LS} L_{\mu_L} \tilde{H} (\mathbf{Y}_3^{(-2)} S_L^c)_{1'} + \gamma_{LS} L_{\tau_L} \tilde{H} (\mathbf{Y}_3^{(-2)} S_L^c)_{1''} \right] \frac{\phi}{\Lambda} + \text{h.c.}, \quad (3.5)$$

where, the choice of the Yukawa coupling is $\mathbf{Y}_3^{(-2)} = (Y_{3,1}^{(-2)}, Y_{3,2}^{(-2)}, Y_{3,3}^{(-2)})$ (expressions can be found in Appendix A Eqn. A.4, A.5, A.6) to keep the Lagrangian invariant with the subscript for the operator $(\mathbf{Y}_3^{(-2)} S_L^c)$ indicates A_4 representation constructed by its product rule and $\{\alpha_{LS}, \beta_{LS}, \gamma_{LS}\}$ are free parameters with $\tilde{x} = \frac{x}{\alpha_{LS}}$ (i.e. $x = \beta_{LS}, \gamma_{LS}$). The flavor structure for the pseudo-Dirac neutrino mass matrix takes the form,

$$M_{LS} = \frac{v_H}{\sqrt{2}} \left(\frac{v_\phi}{\sqrt{2}\Lambda} \right) \alpha_{LS} \begin{bmatrix} 1 & 0 & 0 \\ 0 & \tilde{\beta}_{LS} & 0 \\ 0 & 0 & \tilde{\gamma}_{LS} \end{bmatrix} \begin{bmatrix} Y_{3,1}^{(-2)} & Y_{3,3}^{(-2)} & Y_{3,2}^{(-2)} \\ Y_{3,3}^{(-2)} & Y_{3,2}^{(-2)} & Y_{3,1}^{(-2)} \\ Y_{3,2}^{(-2)} & Y_{3,1}^{(-2)} & Y_{3,3}^{(-2)} \end{bmatrix}_{LR} \quad (3.6)$$

where v_ϕ is the VEV of ϕ , i.e., $\langle \phi \rangle = v_\phi/\sqrt{2}$.

3.3 Mixing between the heavy fields N_R and S_L^c

Following the transformation of the heavy fields under the imposed symmetries, one can have the interactions leading to the mixing between these additional fields as follows

$$\mathcal{L}_{M_{RS}} = [\alpha_{NS} \mathbf{Y}_3^{(-2)} (S_L^c N_R)_{\text{sym}} + \beta_{NS} \mathbf{Y}_3^{(-2)} (S_L^c N_R)_{\text{Anti-sym}}] \phi + \text{h.c.} \quad (3.7)$$

where the first and second terms in (3.7) correspond to symmetric and anti-symmetric product for $S_L^c N_R$, making triplet representation of A_4 with α_{NS} , β_{NS} being the free parameters with $\tilde{\beta}_{NS} = \beta_{NS}/\alpha_{NS}$. Thus, the resulting mass matrix is found to be,

$$M_{RS} = \frac{v_\phi}{\sqrt{2}} \alpha_{NS} \left(\frac{1}{3} \begin{bmatrix} 2Y_{3,1}^{(-2)} & -Y_{3,3}^{(-2)} & -Y_{3,2}^{(-2)} \\ -Y_{3,3}^{(-2)} & 2Y_{3,2}^{(-2)} & -Y_{3,1}^{(-2)} \\ -Y_{3,2}^{(-2)} & -Y_{3,1}^{(-2)} & 2Y_{3,3}^{(-2)} \end{bmatrix} + \tilde{\beta}_{NS} \begin{bmatrix} 0 & Y_{3,3}^{(-2)} & -Y_{3,2}^{(-2)} \\ -Y_{3,3}^{(-2)} & 0 & Y_{3,1}^{(-2)} \\ Y_{3,2}^{(-2)} & -Y_{3,1}^{(-2)} & 0 \end{bmatrix} \right). \quad (3.8)$$

It should be noted that $1/3 \neq \tilde{\beta}_{NS}$, otherwise the matrix M_{NS} becomes singular, which eventually spoils the intent of the linear seesaw.

3.4 Majorana term for N_R

The Majorana mass term for N_R is allowed in this framework, which can be obtained from the Lagrangian.

$$\mathcal{L}_N = \frac{M_R}{2} \left(\alpha_R (N_R \overline{N_R^c}) Y_3^{(0)} + \beta_R (N_R \overline{N_R^c}) Y_1^{(0)} \right) + \text{h.c.} \quad (3.9)$$

and is expressed as

$$M_N = M_R \alpha_R \begin{pmatrix} 2Y_{3,1}^{(0)} + \tilde{\beta}_R & -Y_{3,3}^{(0)} & -Y_{3,2}^{(0)} \\ -Y_{3,3}^{(0)} & 2Y_{3,2}^{(0)} & -Y_{3,1}^{(0)} + \tilde{\beta}_R \\ -Y_{3,2}^{(0)} & -Y_{3,1}^{(0)} + \tilde{\beta}_R & 2Y_{3,3}^{(0)} \end{pmatrix}. \quad (3.10)$$

with $Y_1^{(0)} = 1$ and $\tilde{\beta}_R = \beta_R/\alpha_R$.

3.5 Linear Seesaw mechanism for light neutrino masses

Within the present model invoked with A_4 modular symmetry, the complete 9×9 mass matrix in the flavor basis of $(\nu_L, N_R, S_L^c)^T$ is given by

$$\mathbb{M} = \left(\begin{array}{c|ccc} & \nu_L & N_R & S_L^c \\ \hline \nu_L & 0 & M_D & M_{LS} \\ N_R & M_D^T & M_N & M_{RS} \\ S_L^c & M_{LS}^T & M_{RS}^T & 0 \end{array} \right), \quad (3.11)$$

The effective light neutrino mass matrix can be obtained by block diagonalizing Eq. (3.11). In the linear seesaw framework, the expansion is performed under the hierarchical regime

$$M_{LS} \ll M_D \ll M_{RS}, \quad M_N \ll M_{RS}, \quad (3.12)$$

where the heavy (N_R, S_L^c) block is dominated by M_{RS} and the lepton number violating terms M_{LS} and M_N are expected to be naturally small. This ensures that the eigenvalues of the heavy sector are of $\mathcal{O}(M_{RS})$, justifying the seesaw expansion.

Block diagonalization of Eq. (3.11) (see Appendix B), yields the effective light neutrino mass matrix, having the form

$$m_\nu = M_D(M_{LS}M_{RS}^{-1})^T + (M_{LS}M_{RS}^{-1})M_D^T - M_{LS}M_{RS}^{-1}M_N(M_{RS}^T)^{-1}M_{LS}^T. \quad (3.13)$$

Under the hierarchical conditions mentioned in Eq. (3.12), the last term in (3.13) turns out to be of the form of double seesaw and is considerably suppressed with respect to the first two terms and acts as a higher-order correction, which can be safely ignored.

Thus, retaining only the leading contribution, the light neutrino mass matrix takes the linear seesaw form

$$m_\nu \simeq M_D M_{RS}^{-1} M_{LS}^T + \text{transpose} = \left[\frac{v_H^2 \alpha_D \alpha_{LS}}{2 \Lambda \alpha_{RS}} \right] \tilde{m}_\nu = \kappa \tilde{m}_\nu, \quad (3.14)$$

where $\kappa = \frac{v_H^2 \alpha_D \alpha_{LS}}{2 \Lambda \alpha_{RS}}$ sets the overall mass scale and \tilde{m}_ν is a dimensionless 3×3 matrix. The Hermitian matrix $\tilde{m}_\nu^\dagger \tilde{m}_\nu$ is diagonalized by a unitary matrix V_ν as

$$V_\nu^\dagger \left(\tilde{m}_\nu^\dagger \tilde{m}_\nu \right) V_\nu = \text{diag} \left(\tilde{D}_{\nu_1}^2, \tilde{D}_{\nu_2}^2, \tilde{D}_{\nu_3}^2 \right), \quad V_\nu^\dagger V_\nu = 1_{3 \times 3}. \quad (3.15)$$

The overall scale κ is fixed by the atmospheric mass-squared difference:

$$\text{(NO)} : \quad \kappa^2 = \frac{|\Delta m_{\text{atm}}^2|}{\tilde{D}_{\nu_3}^2 - \tilde{D}_{\nu_1}^2}, \quad \text{(IO)} : \quad \kappa^2 = \frac{|\Delta m_{\text{atm}}^2|}{\tilde{D}_{\nu_2}^2 - \tilde{D}_{\nu_3}^2}, \quad (3.16)$$

where NO (IO) denotes normal (inverted) ordering. The solar mass-squared difference is then given by

$$\Delta m_{\text{sol}}^2 = \kappa^2 \left(\tilde{D}_{\nu_2}^2 - \tilde{D}_{\nu_1}^2 \right), \quad (3.17)$$

which can be compared with the observed value.

3.6 Neutrino Oscillation Observables

Neutrino oscillations are described by six physical observables: the two mass-squared differences Δm_{sol}^2 and Δm_{atm}^2 , three mixing angles θ_{12} , θ_{23} , θ_{13} , and the Dirac CP phase δ_{CP} . The mass-squared splittings are defined as $\Delta m_{\text{sol}}^2 = m_2^2 - m_1^2$ for both normal ordering (NO) and inverted ordering (IO), while $\Delta m_{\text{atm}}^2 = m_3^2 - m_1^2$ for NO and $\Delta m_{\text{atm}}^2 = m_2^2 - m_3^2$ for IO. The leptonic mixing angles are extracted from the elements of the PMNS matrix as

$$\sin^2 \theta_{12} = \frac{|U_{e2}|^2}{1 - |U_{e3}|^2}, \quad (3.18)$$

$$\sin^2 \theta_{23} = \frac{|U_{\mu 3}|^2}{1 - |U_{e3}|^2}, \quad (3.19)$$

$$\sin^2 \theta_{13} = |U_{e3}|^2, \quad (3.20)$$

while the Dirac CP phase can be determined through the rephasing-invariant product $U_{e2}U_{\mu3}U_{e3}^*U_{\mu2}^*$ of the PMNS matrix elements. The allowed parameter space is obtained by fitting these inputs to the six neutrino oscillation observables using results from global analyses [101–103]. The corresponding best-fit values and 3σ ranges are summarized in Table 3. Apart from the smallness of neutrino masses, another important observable in the neutrino sector includes the Jarlskog invariant, which quantifies CP violation in neutrino oscillations and can be expressed in terms of the mixing angles and CP-violating phases of the PMNS matrix as

$$J_{CP} = \text{Im}[U_{e1}U_{\mu2}U_{e2}^*U_{\mu1}^*] = \sin\theta_{23}\cos\theta_{23}\sin\theta_{12}\cos\theta_{12}\sin\theta_{13}\cos^2\theta_{13}\sin\delta_{CP}. \quad (3.21)$$

Parameters	Normal ordering		Inverted ordering	
	Best-fit value	3σ range	Best-fit value	3σ range
$\sin^2\theta_{12}$	$0.308^{+0.012}_{-0.011}$	0.275 – 0.345	$0.308^{+0.012}_{-0.011}$	0.275 – 0.345
$\sin^2\theta_{23}$	$0.470^{+0.017}_{-0.013}$	0.435 – 0.585	$0.550^{+0.012}_{-0.015}$	0.440 – 0.584
$\sin^2\theta_{13}$	$0.02215^{+0.00056}_{-0.00058}$	0.02030 – 0.02388	$0.02231^{+0.00056}_{-0.00056}$	0.02060 – 0.02409
$\frac{\Delta m_{\text{sol}}^2}{10^{-5}\text{eV}^2}$	$7.49^{+0.19}_{-0.19}$	6.92 – 8.05	$7.49^{+0.19}_{-0.19}$	6.92 – 8.05
$\frac{\Delta m_{\text{atm}}^2}{10^{-3}\text{eV}^2}$	$2.513^{+0.021}_{-0.019}$	2.451 – 2.578	$2.484^{+0.020}_{-0.020}$	2.421 – 2.547
$\delta_{CP}/^\circ$	212^{+26}_{-41}	124 – 364	274^{+22}_{-25}	201 – 335

Table 3. Best-fit values and their 3σ ranges for neutrino oscillation parameters obtained from NuFIT 6.1 [103].

4 Simulation Details

The long-baseline simulations are performed using the GLoBES framework [104, 105]. For the DUNE setup, we employ the official configuration files corresponding to the Technical Design Report (TDR) [106]. DUNE is a next-generation accelerator-based neutrino oscillation experiment based at Fermilab (USA), with a far detector located in South Dakota. The experiment utilizes a high-intensity neutrino beam with a nominal beam power of 1.2 MW and covers a broad neutrino energy range. The far detector consists of a 40 kt liquid argon time projection chamber (LArTPC), while the near detector complex is situated at Fermilab to characterize the beam.

In our analysis, we assume a total exposure of 13 years, divided equally between neutrino and antineutrino modes (6.5 years each). This corresponds to an annual exposure of 1.1×10^{21} protons on target (PoT). The adopted configuration is consistent with the nominal staging scenario described in Ref. [107].

The experimental sensitivity is evaluated through a χ^2 analysis based on the Poisson log-likelihood function,

$$\chi_{\text{stat}}^2 = 2 \sum_{i=1}^n \left[N_i^{\text{test}} - N_i^{\text{true}} - N_i^{\text{true}} \ln \left(\frac{N_i^{\text{test}}}{N_i^{\text{true}}} \right) \right], \quad (4.1)$$

Systematics	DUNE
Sg-norm ν_e	2%
Sg-norm ν_μ	5%
Bg-norm	5% to 20%

Table 4. Systematic uncertainties considered in the DUNE simulation. Here “Sg” and “Bg” denote signal and background contributions, respectively, while “norm” refers to normalization uncertainties.

where N_i^{true} and N_i^{test} denote the predicted event rates in the i^{th} energy bin for the true and test hypotheses, respectively, and n represents the total number of bins.

Systematic uncertainties are incorporated using the pull method [108, 109]. In our implementation, both signal and background normalization uncertainties are included, along with shape uncertainties where applicable. The systematic inputs adopted for DUNE are summarized in Table 4.

The oscillation parameters are taken from the latest global fit results of NuFit 6.1 [103], listed in Table 3. During the statistical analysis, we marginalize over the oscillation parameters within the ranges predicted by the underlying model.

To assess the compatibility of the model predictions with the NuFit 6.1 results, we compute an additional χ^2 defined as

$$\chi^2 = \sum_i \frac{(O_i^{\text{Th}} - O_i^{\text{Exp}})^2}{\sigma_i^2}, \quad (4.2)$$

where O_i^{Th} and O_i^{Exp} denote the theoretical and experimental central values of the i^{th} observable, respectively, and σ_i corresponds to the associated experimental uncertainty.

5 Results

In this section, we identify the allowed region of our model parameter space consistent with neutrino oscillation data at the 3σ level, see Tab. 3. Recall that in our setup, we have 5 free parameters and the modulus τ . In our scan, τ is varied within the fundamental domain defined by

$$\left| \text{Re}(\tau) \right| \in [0, 0.5], \quad \text{Im}(\tau) \in [0.86, 5.0], \quad (5.1)$$

while the ratio of the free parameters are taken to be in the range

$$\tilde{\beta}_D, \tilde{\beta}_{LS}, \tilde{\gamma}_D, \tilde{\gamma}_{LS}, \tilde{\beta}_{NS} \in [10^{-3}, 10^3]. \quad (5.2)$$

For fitting the neutrino oscillation observables and we make use of a package Flavorpy [110].

5.1 Predictions from the model

Our model accommodates both Normal Ordering (NO) and Inverted Ordering (IO) of neutrino masses for phenomenologically viable values of the complex modulus parameter

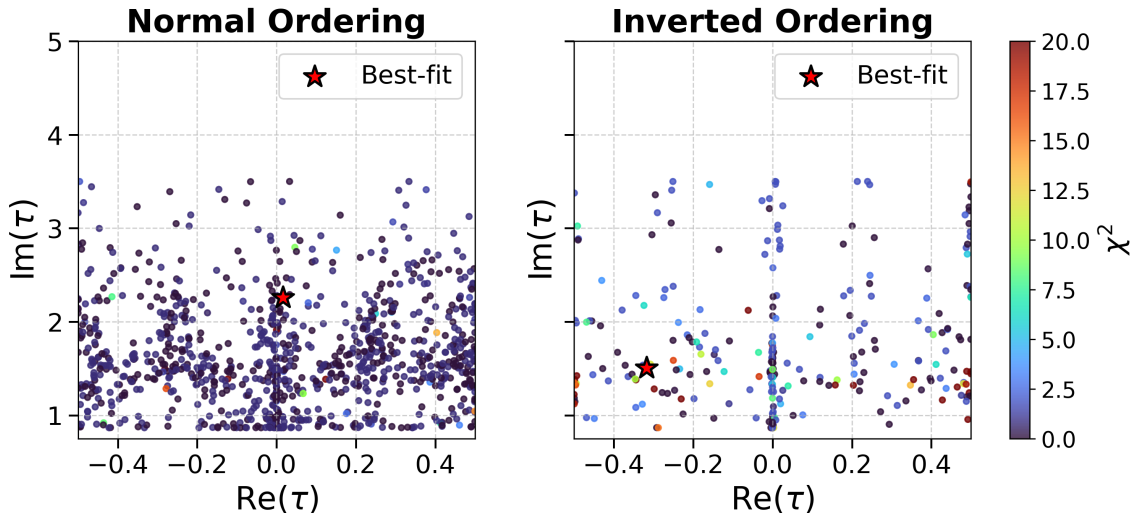


Figure 1. Parameter space between $\text{Re}(\tau)$ and $\text{Im}(\tau)$ for the model preferring NO and IO in left and right panel, respectively. The colour regions represent the different χ^2 values.

τ . The allowed regions in the complex τ -plane are shown in Fig. 1, where we scan the parameter space by varying $\text{Re}(\tau)$ in the range $[-0.5, 0.5]$ and $\text{Im}(\tau)$ in the range $[0.86, 5]$. Best fit points are shown with a red asterisk symbol, and the corresponding best-fit values of $\text{Re}(\tau)$ and $\text{Im}(\tau)$ are summarized in Table 5. For the normal ordering case, the analysis yields best-fit values $\text{Re}(\tau) = 0.02$ and $\text{Im}(\tau) = 2.26$. In contrast, for the inverted ordering scenario, the model prefers comparatively smaller values of the modulus parameters, with $\text{Re}(\tau) = -0.32$ and $\text{Im}(\tau) = 1.5$.

Parameters	Normal Ordering (NO)		Inverted Ordering (IO)	
	Best fit	Parameter range	Best fit	Parameter range
$\text{Re}(\tau)$	0.02	$[-0.5, 0.5]$	-0.32	$[-0.5, 0.5]$
$\text{Im}(\tau)$	2.26	$[0.86, 5]$	1.5	$[0.86, 5]$

Table 5. Best fit values of the parameter from the model for NO and IO.

Varying the value of τ within the range given in Table 5, we obtain the allowed parameter regions among $\sin^2 \theta_{13}$, $\sin^2 \theta_{23}$, Δm_{31}^2 , and δ_{CP} , as shown in Figs. 2 and 3. The left panels correspond to the NO, while the right panels correspond to the IO. The scattered points represent the parameter space allowed by the model, and the color bar indicates the corresponding χ^2 values of the data points. The 2σ and 3σ NuFIT regions are indicated by the green shaded bands. The solid and dashed contours depict the allowed parameter space of the DUNE experiment. Here, we compare the parameter space predicted by the model with the parameter-constrained regions expected from DUNE. Our model allows δ_{CP} within the full range $[0, 360^\circ]$ and $\sin^2 \theta_{23}$ within $[0.44, 0.60]$. The predicted values of $\sin^2 \theta_{13}$ and Δm_{31}^2 lie within the region allowed by NuFIT.

The allowed regions for the DUNE experiment shown in Fig. 2 are obtained by minimizing over the oscillation parameters θ_{23} , Δm_{31}^2 , and δ_{CP} , except when the corresponding

parameter space is explicitly displayed. From Fig. 2, it is evident that DUNE will strongly constrain θ_{23} , δ_{CP} , and Δm_{31}^2 , whereas it has limited sensitivity to θ_{13} . The sensitivity to θ_{13} at DUNE is affected by parameter degeneracies. In contrast, reactor experiments such as Daya Bay, RENO, and Double Chooz provide high-precision measurements of θ_{13} .

The model constrains $\sin^2 \theta_{13}$ to lie in the range 0.022–0.024 for NO and 0.020–0.024 for IO. The parameter space predicted by the model in the Δm_{31}^2 – $\sin^2 \theta_{13}$ plane (upper panel of Fig. 2) lies within the 3σ allowed regions of both the NuFIT data and the DUNE experiment for both NO and IO scenarios. The parameter space in the $\sin^2 \theta_{13}$ – $\sin^2 \theta_{23}$ plane exhibits interesting features: for NO, $\sin^2 \theta_{23}$ shows degenerate solutions around ~ 0.47 and ~ 0.56 . In the IO scenario, the allowed region includes additional parameter space around $\sin^2 \theta_{23} \sim 0.46$ and ~ 0.55 . Furthermore, the model permits the full range of δ_{CP} values within $[0, 360^\circ]$.

Fig. 3 illustrates the allowed parameter space in the $\sin^2 \theta_{23}$, δ_{CP} , and Δm_{31}^2 planes. The NuFIT best-fit values are indicated by asterisks. The left panels correspond to NO, while the right panels represent IO. The upper panels display the allowed regions in the Δm_{31}^2 – δ_{CP} plane. For both NO and IO, the model accommodates δ_{CP} across the full interval $[0, 360^\circ]$, while Δm_{31}^2 is restricted to approximately $[2.46 - 2.50] \times 10^{-3} \text{ eV}^2$. The model-predicted parameter space lies within the 3σ region allowed by NuFIT. The projected sensitivity of DUNE significantly constrains the Δm_{31}^2 – δ_{CP} parameter space, and a subset of the model-preferred points falls within the 3σ contour of DUNE experiment.

The middle panels show the allowed regions in the Δm_{31}^2 – $\sin^2 \theta_{23}$ plane. The preferred ranges obtained from the model are consistent with the global oscillation analysis of NuFIT. Although $\sin^2 \theta_{23}$ spans the interval $[0.4, 0.6]$, the model exhibits a pronounced preference near $\sin^2 \theta_{23} \simeq 0.47$ for NO and $\sin^2 \theta_{23} \simeq 0.55$ for IO. Degenerate solutions are observed in both orderings, reflecting the well-known octant degeneracy. The spread of the NuFIT-allowed region corresponds to the coexistence of lower and higher-octant solutions. The DUNE sensitivity projections demonstrate a substantial reduction of the allowed parameter space, indicating its capability to resolve the octant–hierarchy degeneracy. A non-negligible fraction of the model predictions overlaps with the 3σ DUNE sensitivity region.

The lower panels present the allowed parameter space in the δ_{CP} – $\sin^2 \theta_{23}$ plane. The model permits δ_{CP} throughout $[0, 360^\circ]$ and $\sin^2 \theta_{23}$ within $[0.4, 0.6]$, with enhanced prediction density around $\sin^2 \theta_{23} \approx 0.47$ and 0.55 . In contrast, the DUNE projections indicate a significantly narrower allowed region. Overall, the model predictions are compatible with the current NuFIT constraints and partially fall within the projected sensitivity reach of DUNE.

5.2 Neutrinoless Double Beta Decay

In this section, we have shown the model’s capability to predict the effective electron neutrino mass, the effective Majorana neutrino mass, and the sum of neutrino masses.

The effective mass of the electron neutrino can be determined from the endpoint energy

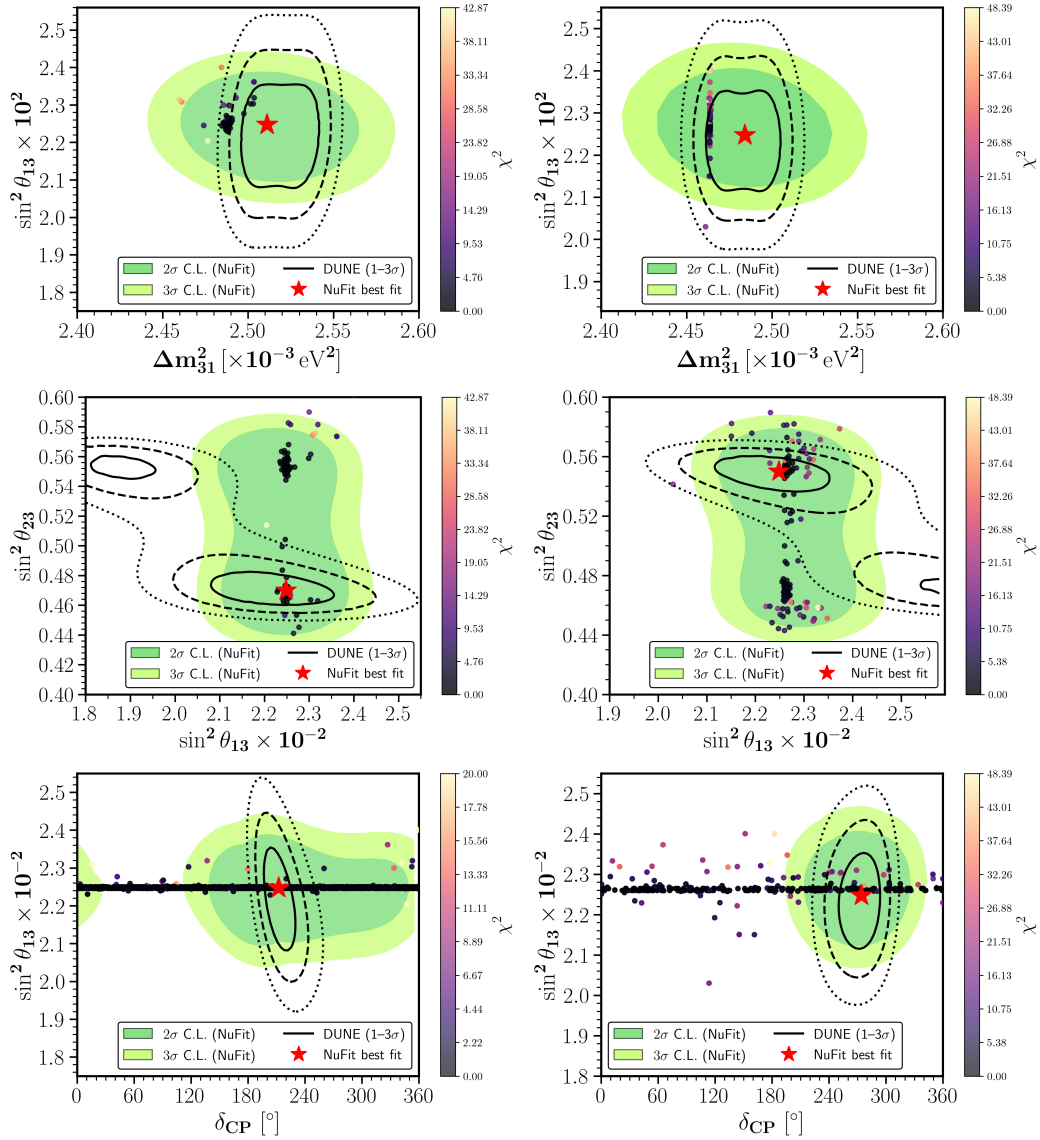


Figure 2. Allowed parameter spaces among the oscillation parameters for normal ordering (NO, left panel) and inverted ordering (IO, right panel). The contour lines indicate the allowed regions from the DUNE experiment, while the green contours show the NuFIT constraints. The scattered points correspond to the parameter space permitted by the model.

of the beta decay spectrum and can be written as

$$m_{\nu_e}^{\text{eff}} = \sqrt{\sum_i |U_{ei}|^2 m_i^2} \quad (5.3)$$

where U_{ei} is the mixing matrix elements and m_i is the mass of neutrino. The left panel of Fig. 4 shows the effective neutrino mass $m_{\nu_e}^{\text{eff}}$ predicted by the model for NO and IO, with red and blue points, respectively. The gray shaded region shows the region disfavored by cosmological data. Experimental data from KATRIN put constraints on $m_{\nu_e}^{\text{eff}} < 0.45$ eV at

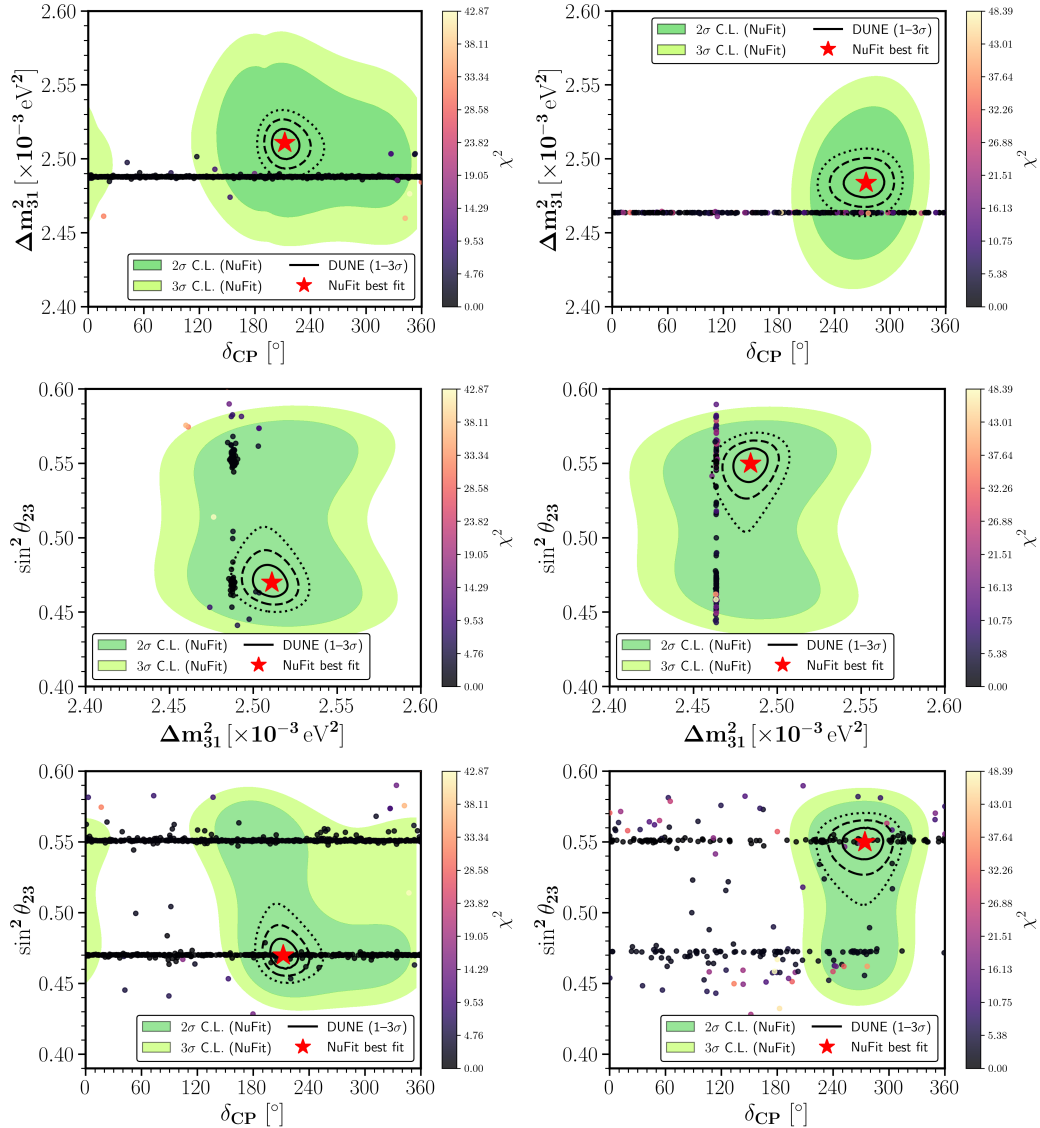


Figure 3. Allowed parameter spaces between $\sin^2 \theta_{23}$, Δm_{31}^2 and δ_{CP} by the Models preferring NO (in left panel) and IO (in right panel). The contour lines denote the allowed regions from the DUNE experiment. The green contours correspond to the parameter space from NuFIT, while the scattered points represent the region allowed by the model.

90% C.L. [111]. Project 8 can also put very stringent upper bounds on $m_{\nu_e}^{\text{eff}} < 0.04$ eV [112]. In the NO case, the entire model-predicted parameter space for $m_{\nu_e}^{\text{eff}} \simeq 0.008\text{--}0.015$ eV remains below the expected sensitivity of the Project 8 experiment. For the IO case, the predicted model parameter space $m_{\nu_e}^{\text{eff}} \simeq 0.045\text{--}0.060$ eV lies above the Project 8 sensitivity limit (i.e. $m_{\nu_e}^{\text{eff}} > 0.04\text{eV}$).

Neutrinoless double beta decay ($0\nu\beta\beta$) may shed light on the Majorana nature of

neutrinos. The half-life of $0\nu\beta\beta$ process can be expressed as

$$T_{1/2}^{-1} \simeq G_{0\nu} \left| \frac{\mathcal{M}_N}{m_e} \right|^2 |m_{\beta\beta}|^2, \quad (5.4)$$

where $G_{0\nu}$ is phase space factor, m_e is the mass of electron, \mathcal{M}_N is the nuclear matrix elements for the nucleus, and $|m_{\beta\beta}|$ is the absolute effective Majorana mass parameter. The effective Majorana mass parameter can be characterized in terms of the PMNS mixing matrix elements as

$$|m_{\beta\beta}| = |m_1|U_{e1}|^2 + m_2|U_{e2}|^2 e^{i\alpha_{21}} + m_3|U_{e3}|^2 e^{i(\alpha_{31}-2\delta_{CP})}, \quad (5.5)$$

where the m_i 's are the neutrino masses and U_{ei} 's are the mixing matrix elements associated with electron with ($i = 1, 2, 3$), which depend upon the mixing angles. Phases α_{21} and α_{31} are the Majoran phases and δ_{CP} is the Dirac CP phase. Many dedicated experiments are looking for neutrinoless double beta signals; for details, please refer to [113]. The sensitivity limits on $|m_{\beta\beta}|$ by the current experiments such as GERDA is (102 – 213) meV [114] and CUORE is (90 – 420) meV [115]. The recent result of KamLAND-Zen experiment constraints $m_{\beta\beta} < (28 - 122)$ meV [116]. The future generation experiments, like LEGEND-1000 can probe 9 – 21 meV [117] and nEXO can reach 4.7 – 20.3 meV in the future [118]. In Fig. 4 (right panel), we have shown the $m_{\beta\beta}$ as a function of lightest neutrino mass. We present the predictions of our model as data points in blue and red for the NO and IO cases, respectively. The light-blue and light-red shaded regions represent the theoretical allowed NO and IO parameter space, respectively. The horizontal gray shaded band corresponds to the region disfavored by $0\nu\beta\beta$ searches, while the vertical shaded band indicates the region excluded by cosmological constraints.

For both the mass ordering case, the majority of the parameter space predicted by the model falls within the corresponding theoretical region. For NO, the predicted values of $m_{\beta\beta} \simeq 0.0008-0.04$ eV lie below the present experimental bounds from LEGEND and KamLAND-Zen, although a part of the parameter space remains within the projected sensitivity of the nEXO experiment. In contrast, for IO, the predicted values of $m_{\beta\beta} \simeq 0.017-0.061$ eV fall within the future discovery reach of nEXO and LEGEND, while still remaining below the current observational sensitivity of KamLAND-Zen experiment.

Figure 5 shows the sum of neutrino masses as a function of the lightest neutrino mass. The Planck measurement of the cosmic microwave background (CMB) for cosmological parameters provides a stringent constraint on the sum of neutrino masses, $\sum m_\nu < 0.12$ eV [119]. A recent result from the DESI Collaboration reports that the combined analysis of DESI BAO and CMB data sets a tighter upper bound, $\sum m_\nu < 0.072$ eV [120]. In the future, the joint analysis of Euclid, CMB-S4, and LiteBIRD data is expected to measure $\sum m_\nu$ in the range (0.044 – 0.076) eV [121]. The model prediction for $\sum m_\nu$ for the NO scenario lies below the upper limit of Planck + Lensing + BAO data. Most of the predicted data in IO case is above the upper limit of Planck + Lensing + BAO data. However, the prediction in the case of IO lie in $\sum m_\nu \simeq 0.10-0.16$ eV, exceeds the futuristic upper limit of Euclid, CMB-S4, and LiteBIRD experiments. The range of prediction for

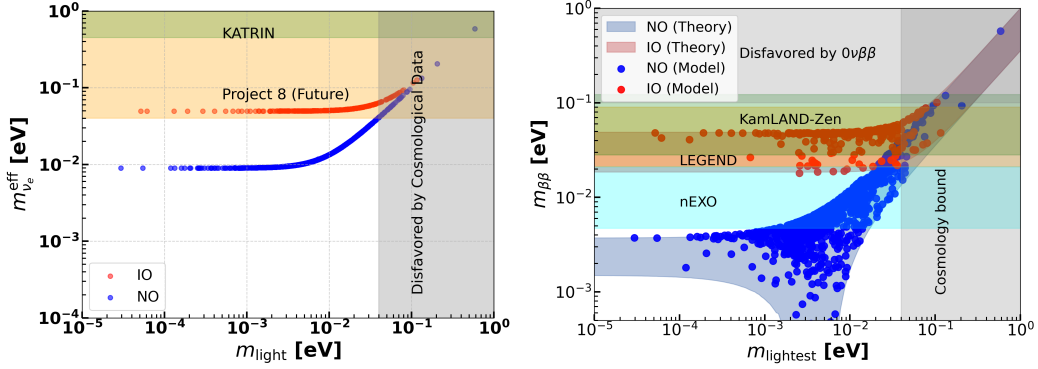


Figure 4. Effective Majorana mass for neutrino $m_{\beta\beta}$ (right panel) and m_ν (left panel) as a function of lightest neutrino mass for NO and IO, allowed by the model.

$\sum m_\nu \simeq 0.058\text{--}0.13$ eV in NO is within the expected sensitivity range of Euclid+ CMB-S4, + LiteBIRD limit.

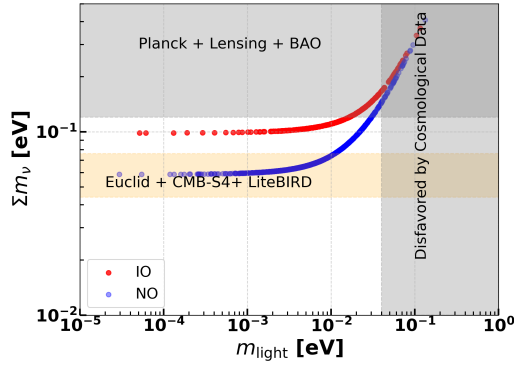


Figure 5. Sum of neutrino masses $\sum m_i$ as a function of lightest neutrino mass for NO and IO, allowed by the model.

6 Summary and Conclusions

In this work, we have presented a predictive realization of the linear seesaw mechanism within a non-holomorphic modular A_4 flavor symmetry framework using polyharmonic Maaß modular forms in a non-supersymmetric setup. The model introduces six gauge-singlet fermions (N_R, S_L) together with a single flavon field, thereby significantly reducing scalar-sector arbitrariness compared to conventional A_4 constructions and earlier holomorphic modular linear seesaw models. Once the modulus τ acquires a vacuum expectation value in the fundamental domain, the entire flavor structure is dynamically fixed. Under the hierarchy $M_{LS} \ll M_D \ll M_{RS}$ with $M_N \ll M_{RS}$, the effective light neutrino mass matrix naturally assumes the linear seesaw structure with dominant scaling $m_\nu \sim M_D M_{LS} / M_{RS}$. Our numerical scan reveals viable solutions for $\text{Re}(\tau) \in [-0.5, 0.5]$ and $\text{Im}(\tau) \in [0.86, 5]$ in the NO case, while the IO solutions are more restricted, cluster-

ing around $\text{Re}(\tau) \approx 0$ and $\text{Im}(\tau)$ spans in a wider parameter space. For NO, the model predicts $\sin^2 \theta_{12} \simeq 0.27\text{--}0.35$, $\sin^2 \theta_{13} \simeq 0.020\text{--}0.024$, and $\sin^2 \theta_{23} \simeq 0.46\text{--}0.48$ or $0.53\text{--}0.56$, clearly exhibiting an octant degeneracy. The atmospheric mass squared difference lie in the range $|\Delta m_{31}^2| \simeq (2.45\text{--}2.5) \times 10^{-3} \text{ eV}^2$. In the IO scenario, the allowed region is comparatively compressed around $\sin^2 \theta_{23} \simeq 0.47$ and 0.55 , and $|\Delta m_{31}^2| \simeq 2.46 \times 10^{-3} \text{ eV}^2$, while the Dirac CP phase δ_{CP} spans nearly the full physical range $[0, 2\pi]$. In the absolute neutrino mass sector, we obtain $\sum m_\nu \simeq 0.058\text{--}0.13 \text{ eV}$ for NO and $\sum m_\nu \simeq 0.10\text{--}0.16 \text{ eV}$ for IO, placing much of the IO parameter space close to present cosmological bounds. The effective electron neutrino mass is predicted to be $m_{\nu_e}^{\text{eff}} \simeq 0.008\text{--}0.015 \text{ eV}$ in NO and $m_{\nu_e}^{\text{eff}} \simeq 0.045\text{--}0.060 \text{ eV}$ in IO. The effective Majorana mass relevant for neutrinoless double beta decay lies in the ranges $m_{\beta\beta} \simeq 0.0008\text{--}0.04 \text{ eV}$ for NO and $m_{\beta\beta} \simeq 0.017\text{--}0.061 \text{ eV}$ for IO, with the IO region significantly overlapping the projected sensitivities of next-generation experiments. Furthermore, our GLoBES-based simulation of DUNE indicates that future precision measurements will substantially reduce the allowed parameter space in the $(\theta_{23}, \delta_{\text{CP}})$ and $(\Delta m_{31}^2, \delta_{\text{CP}})$ planes, potentially resolving the octant degeneracy predicted by the model. Overall, the non-holomorphic modular A_4 linear seesaw framework provides a theoretically economical and symmetry-driven description of neutrino mass generation, yielding sharply defined numerical predictions and distinctive parameter correlations that can be tested in upcoming oscillation, cosmological, and neutrinoless double beta decay experiments.

A Modular Yukawa couplings

The functions $Y_{3,i}^{(0)}$ and $Y_{3,i}^{(-2)}$ ($i = 1, 2, 3$) are modular Yukawa couplings transforming as an A_4 triplet with modular weights 0 and -2 , respectively, expressed in terms of the modulus $\tau = x + iy$ and $q = e^{2\pi i\tau}$. Their q -expansions are given as follows:

$$Y_{3,1}^{(0)} = y - \frac{3e^{-4\pi y}}{\pi q} - \frac{9e^{-8\pi y}}{2\pi q^2} - \frac{e^{-12\pi y}}{\pi q^3} - \frac{21e^{-16\pi y}}{4\pi q^4} - \frac{18e^{-20\pi y}}{5\pi q^5} - \frac{3e^{-24\pi y}}{2\pi q^6} + \dots$$

$$- \frac{9 \log 3}{4\pi} - \frac{3q}{2\pi} - \frac{9q^2}{2\pi} - \frac{q^3}{\pi} - \frac{21q^4}{4\pi} - \frac{18q^5}{5\pi} - \frac{3q^6}{2\pi} + \dots, \quad (\text{A.1})$$

$$Y_{3,2}^{(0)} = \frac{27q^{1/3}e^{\pi y/3}}{\pi} \left(\frac{e^{-3\pi y}}{4q} + \frac{e^{-7\pi y}}{5q^2} + \frac{5e^{-11\pi y}}{16q^3} + \frac{2e^{-15\pi y}}{11q^4} + \frac{2e^{-19\pi y}}{7q^5} + \frac{4e^{-23\pi y}}{17q^6} + \dots \right)$$

$$+ \frac{9q^{1/3}}{2\pi} \left(1 + \frac{7q}{4} + \frac{8q^2}{7} + \frac{9q^3}{5} + \frac{14q^4}{13} + \frac{31q^5}{16} + \frac{20q^6}{19} + \dots \right), \quad (\text{A.2})$$

$$Y_{3,3}^{(0)} = \frac{9q^{2/3}e^{2\pi y/3}}{2\pi} \left(\frac{e^{-2\pi y}}{q} + \frac{7e^{-6\pi y}}{4q^2} + \frac{8e^{-10\pi y}}{7q^3} + \frac{9e^{-14\pi y}}{5q^4} + \frac{14e^{-18\pi y}}{13q^5} + \frac{31e^{-22\pi y}}{16q^6} + \dots \right)$$

$$+ \frac{27q^{2/3}}{\pi} \left(\frac{1}{4} + \frac{q}{5} + \frac{5q^2}{16} + \frac{2q^3}{11} + \frac{2q^4}{7} + \frac{9q^5}{17} + \frac{21q^6}{20} + \dots \right). \quad (\text{A.3})$$

$$\begin{aligned}
Y_{3,1}^{(-2)}(\tau) &= \frac{y^3}{3} + \frac{21\Gamma(3, 4\pi y)}{16\pi^3 q} + \frac{189\Gamma(3, 8\pi y)}{128\pi^3 q^2} + \frac{169\Gamma(3, 12\pi y)}{144\pi^3 q^3} + \frac{1533\Gamma(3, 16\pi y)}{1024\pi^3 q^4} + \dots \\
&+ \frac{\pi\zeta(3)}{40\zeta(4)} + \frac{21q}{8\pi^3} + \frac{189q^2}{64\pi^3} + \frac{169q^3}{72\pi^3} + \frac{1533q^4}{512\pi^3} + \frac{1323q^5}{500\pi^3} + \frac{169q^6}{64\pi^3} + \dots,
\end{aligned} \tag{A.4}$$

$$\begin{aligned}
Y_{3,2}^{(-2)}(\tau) &= -\frac{729q^{1/3}}{16\pi^3} \left(\frac{\Gamma(3, 8\pi y/3)}{16q} + \frac{7\Gamma(3, 20\pi y/3)}{125q^2} + \frac{65\Gamma(3, 32\pi y/3)}{1024q^3} + \frac{74\Gamma(3, 44\pi y/3)}{1331q^4} + \dots \right) \\
&- \frac{81q^{1/3}}{16\pi^3} \left(1 + \frac{73q}{64} + \frac{344q^2}{343} + \frac{567q^3}{500} + \frac{20198q^4}{2197} + \frac{4681q^5}{4096} + \dots \right),
\end{aligned} \tag{A.5}$$

$$\begin{aligned}
Y_{3,3}^{(-2)}(\tau) &= -\frac{81q^{2/3}}{32\pi^3} \left(\frac{\Gamma(3, 4\pi y/3)}{q} + \frac{73\Gamma(3, 16\pi y/3)}{64q^2} + \frac{344\Gamma(3, 28\pi y/3)}{343q^3} + \frac{567\Gamma(3, 40\pi y/3)}{500q^4} + \dots \right) \\
&- \frac{729q^{2/3}}{8\pi^3} \left(\frac{1}{16} + \frac{7q}{125} + \frac{65q^2}{1024} + \frac{74q^3}{1331} + \dots \right).
\end{aligned} \tag{A.6}$$

B Block Diagonalization

For a block matrix M

$$M = \begin{pmatrix} A & B \\ B^T & D \end{pmatrix}, \tag{B.1}$$

where the A , B , and D are $a \times a$, $a \times b$, and $b \times b$ matrices. The dimension of M is $(a+b) \times (a+b)$. Schur complement [122] of the block D when D is invertible is

$$S_D = A - BD^{-1}B^T. \tag{B.2}$$

In this study, the mass matrix in the basis of (ν_l, N_R, S_L^c) basis can be written as

$$M = \begin{pmatrix} 0 & M_D & M_{LS} \\ M_D^T & M_N & M_{RS} \\ M_{LS}^T & M_{RS}^T & 0 \end{pmatrix}. \tag{B.3}$$

The mass matrix M can be block diagonalized through Schur complement using realizing

$$\begin{aligned}
A &= 0, \\
B &= (M_D \ M_{LS}) \\
D &= \begin{pmatrix} M_N & M_{RS} \\ M_{RS}^T & 0 \end{pmatrix},
\end{aligned} \tag{B.4}$$

and the Schur complement as

$$S_D = - \begin{pmatrix} M_D & M_{LS} \end{pmatrix} \begin{pmatrix} 0 & (M_{RS}^T)^{-1} \\ M_{RS}^{-1} & -M_{RS}^{-1}M_N(M_{RS}^T)^{-1} \end{pmatrix} \begin{pmatrix} M_D^T \\ M_{LS}^T \end{pmatrix} \tag{B.5}$$

$$m_\nu = M_D(M_{LS}M_{RS}^{-1})^T + (M_{LS}M_{RS}^{-1})M_D^T - M_{LS}M_{RS}^{-1}M_N(M_{RS}^T)^{-1}M_{LS}^T \tag{B.6}$$

Acknowledgments

RM (Rudra Majhi) would like to acknowledge Odisha State Higher Education Council, Govt. of Odisha for the support under Mukhyamantri Research and Innovation (MRIP)-2024 (24EM/PH/102).

References

- [1] A. Faessler, *Status of the determination of the electron–neutrino mass*, *Prog. Part. Nucl. Phys.* **113** (2020) 103789.
- [2] KATRIN collaboration, *Improved Upper Limit on the Neutrino Mass from a Direct Kinematic Method by KATRIN*, *Phys. Rev. Lett.* **123** (2019) 221802 [[1909.06048](#)].
- [3] B. Pontecorvo, *Neutrino Experiments and the Problem of Conservation of Leptonic Charge*, *Sov. Phys. JETP* **26** (1968) 984.
- [4] F. Feruglio, *Neutrino masses and mixing angles: A tribute to Guido Altarelli*, *Frascati Phys. Ser.* **64** (2017) 174.
- [5] PARTICLE DATA GROUP collaboration, *Review of Particle Physics*, *Phys. Rev.* **D98** (2018) 030001.
- [6] S. Weinberg, *Varieties of Baryon and Lepton Nonconservation*, *Phys. Rev.* **D22** (1980) 1694.
- [7] S. Weinberg, *Baryon and Lepton Nonconserving Processes*, *Phys. Rev. Lett.* **43** (1979) 1566.
- [8] F. Wilczek and A. Zee, *Operator Analysis of Nucleon Decay*, *Phys. Rev. Lett.* **43** (1979) 1571.
- [9] P. Minkowski, *$\mu \rightarrow e\gamma$ at a Rate of One Out of 10^9 Muon Decays?*, *Phys. Lett.* **67B** (1977) 421.
- [10] R.N. Mohapatra and G. Senjanovic, *Neutrino Mass and Spontaneous Parity Nonconservation*, *Phys. Rev. Lett.* **44** (1980) 912.
- [11] M. Gell-Mann, P. Ramond and R. Slansky, *Complex Spinors and Unified Theories*, *Conf. Proc.* **C790927** (1979) 315 [[1306.4669](#)].
- [12] A. Zee, *A Theory of Lepton Number Violation, Neutrino Majorana Mass, and Oscillation*, *Phys. Lett.* **93B** (1980) 389.
- [13] K.S. Babu, *Model of 'Calculable' Majorana Neutrino Masses*, *Phys. Lett.* **B203** (1988) 132.
- [14] N. Arkani-Hamed, S. Dimopoulos, G.R. Dvali and J. March-Russell, *Neutrino masses from large extra dimensions*, *Phys. Rev.* **D65** (2001) 024032 [[hep-ph/9811448](#)].
- [15] R.N. Mohapatra and J.W.F. Valle, *Neutrino Mass and Baryon Number Nonconservation in Superstring Models*, *Phys. Rev.* **D34** (1986) 1642.
- [16] M.C. Gonzalez-Garcia and J.W.F. Valle, *Fast Decaying Neutrinos and Observable Flavor Violation in a New Class of Majoron Models*, *Phys. Lett.* **B216** (1989) 360.
- [17] A. Cárcamo Hernández, J. Marchant González and U. Saldaña-Salazar, *Viable low-scale model with universal and inverse seesaw mechanisms*, *Phys. Rev. D* **100** (2019) 035024 [[1904.09993](#)].

- [18] M. Malinsky, J.C. Romao and J.W.F. Valle, *Novel supersymmetric $SO(10)$ seesaw mechanism*, *Phys. Rev. Lett.* **95** (2005) 161801 [[hep-ph/0506296](#)].
- [19] R.N. Mohapatra et al., *Theory of neutrinos: A White paper*, *Rept. Prog. Phys.* **70** (2007) 1757 [[hep-ph/0510213](#)].
- [20] E. Ma and G. Rajasekaran, *Softly broken $A(4)$ symmetry for nearly degenerate neutrino masses*, *Phys. Rev.* **D64** (2001) 113012 [[hep-ph/0106291](#)].
- [21] H. Ishimori, T. Kobayashi, H. Ohki, H. Okada, Y. Shimizu and M. Tanimoto, *An introduction to non-Abelian discrete symmetries for particle physicists*, vol. 858 (2012), [10.1007/978-3-642-30805-5](#).
- [22] S. Pakvasa and H. Sugawara, *Discrete Symmetry and Cabibbo Angle*, *Phys. Lett. B* **73** (1978) 61.
- [23] F. Feruglio, *Are neutrino masses modular forms?*, in *From My Vast Repertoire ...: Guido Altarelli's Legacy*, pp. 227–266 (2019), DOI [[1706.08749](#)].
- [24] M. Abbas, *Flavor masses and mixing in modular A_4 Symmetry*, [2002.01929](#).
- [25] S.J. King and S.F. King, *Fermion Mass Hierarchies from Modular Symmetry*, [2002.00969](#).
- [26] X. Wang, *Lepton Flavor Mixing and CP Violation in the Minimal Type-(I+II) Seesaw Model with a Modular A_4 Symmetry*, [1912.13284](#).
- [27] J.-N. Lu, X.-G. Liu and G.-J. Ding, *Modular symmetry origin of texture zeros and quark lepton unification*, *Phys. Rev. D* **101** (2020) 115020 [[1912.07573](#)].
- [28] T. Nomura, H. Okada and S. Patra, *An Inverse Seesaw model with A_4 -modular symmetry*, [1912.00379](#).
- [29] T. Asaka, Y. Heo, T.H. Tatsuishi and T. Yoshida, *Modular A_4 invariance and leptogenesis*, *JHEP* **01** (2020) 144 [[1909.06520](#)].
- [30] J. Penedo and S. Petcov, *Lepton Masses and Mixing from Modular S_4 Symmetry*, *Nucl. Phys. B* **939** (2019) 292 [[1806.11040](#)].
- [31] X.-G. Liu, C.-Y. Yao and G.-J. Ding, *Modular Invariant Quark and Lepton Models in Double Covering of S_4 Modular Group*, [2006.10722](#).
- [32] T. Kobayashi, Y. Shimizu, K. Takagi, M. Tanimoto and T.H. Tatsuishi, *A_4 lepton flavor model and modulus stabilization from S_4 modular symmetry*, *Phys. Rev. D* **100** (2019) 115045 [[1909.05139](#)].
- [33] P. Novichkov, J. Penedo, S. Petcov and A. Titov, *Modular S_4 models of lepton masses and mixing*, *JHEP* **04** (2019) 005 [[1811.04933](#)].
- [34] P.P. Novichkov, J.T. Penedo and S.T. Petcov, *Double cover of modular S_4 for flavour model building*, *Nucl. Phys. B* **963** (2021) 115301 [[2006.03058](#)].
- [35] G.-J. Ding, S.F. King, X.-G. Liu and J.-N. Lu, *Modular S_4 and A_4 symmetries and their fixed points: new predictive examples of lepton mixing*, *JHEP* **12** (2019) 030 [[1910.03460](#)].
- [36] G.-J. Ding, S.F. King and X.-G. Liu, *Modular A_4 symmetry models of neutrinos and charged leptons*, *JHEP* **09** (2019) 074 [[1907.11714](#)].
- [37] P. Novichkov, J. Penedo, S. Petcov and A. Titov, *Modular A_5 symmetry for flavour model building*, *JHEP* **04** (2019) 174 [[1812.02158](#)].

- [38] T. Nomura, H. Okada and O. Popov, *A modular A_4 symmetric scotogenic model*, *Phys. Lett. B* **803** (2020) 135294 [[1908.07457](#)].
- [39] E. Ma, *Neutrino mixing: A_4 variations*, *Phys. Lett. B* **752** (2016) 198 [[1510.02501](#)].
- [40] S. Mishra, M. Kumar Behera, R. Mohanta, S. Patra and S. Singirala, *Neutrino Phenomenology and Dark matter in an A_4 flavour extended B-L model*, *Eur. Phys. J. C* **80** (2020) 420 [[1907.06429](#)].
- [41] S. Mishra, M.K. Behera, R. Mohanta, S. Patra and S. Singirala, *Neutrino phenomenology and dark matter in an A_4 flavour extended B – L model*, *Eur. Phys. J. C* **80** (2020) 420 [[1907.06429](#)].
- [42] M.K. Behera, S. Mishra, S. Singirala and R. Mohanta, *Implications of A_4 modular symmetry on neutrino mass, mixing and leptogenesis with linear seesaw*, *Phys. Dark Univ.* **36** (2022) 101027 [[2007.00545](#)].
- [43] M.K. Behera, S. Singirala, S. Mishra and R. Mohanta, *A modular A_4 symmetric scotogenic model for neutrino mass and dark matter*, *J. Phys. G* **49** (2022) 035002 [[2009.01806](#)].
- [44] M.K. Behera and R. Mohanta, *Inverse seesaw in A'_5 modular symmetry*, *J. Phys. G* **49** (2022) 045001 [[2108.01059](#)].
- [45] P. Mishra, M.K. Behera, P. Panda and R. Mohanta, *Type III seesaw under A_4 modular symmetry with leptogenesis*, *Eur. Phys. J. C* **82** (2022) 1115 [[2204.08338](#)].
- [46] P. Mishra, M.K. Behera, P. Panda, M. Ghosh and R. Mohanta, *Exploring models with modular symmetry in neutrino oscillation experiments*, *JHEP* **09** (2023) 144 [[2305.08576](#)].
- [47] R. Kumar, P. Mishra, M.K. Behera, R. Mohanta and R. Srivastava, *Predictions from scoto-seesaw with A_4 modular symmetry*, *Phys. Lett. B* **853** (2024) 138635 [[2310.02363](#)].
- [48] M.K. Behera, P. Ittisamai, C. Pongkitivanichkul and P. Uttayarat, *Neutrino phenomenology in the modular S_3 seesaw model*, *Phys. Rev. D* **110** (2024) 035004 [[2403.00593](#)].
- [49] M.K. Behera, P. Ittisamai, C. Pongkitivanichkul and P. Uttayarat, *Phenomenology of inverse seesaw using S_3 modular symmetry*, *Eur. Phys. J. C* **85** (2025) 1316 [[2504.12954](#)].
- [50] B.-Y. Qu and G.-J. Ding, *Non-holomorphic modular flavor symmetry*, *JHEP* **08** (2024) 136 [[2406.02527](#)].
- [51] Tapender and S. Verma, *Tri-Resonant Leptogenesis in a Non-Holomorphic Modular A_4 Scotogenic Model*, [2602.17243](#).
- [52] S. Nasri, L. Singh, Tapender and S. Verma, *Dark-Portal Leptogenesis in a Non-Holomorphic Modular Scoto-Seesaw Model*, [2601.06435](#).
- [53] Priya, L. Singh, B.C. Chauhan and S. Verma, *Type-III seesaw in non-holomorphic modular symmetry and leptogenesis*, *JHEP* **01** (2026) 036 [[2508.05047](#)].
- [54] T. Nomura and H. Okada, *Type-II seesaw of a non-holomorphic modular A_4 symmetry*, *Phys. Lett. B* **868** (2025) 139763 [[2408.01143](#)].
- [55] T. Nomura, H. Okada and O. Popov, *Non-holomorphic modular A_4 symmetric scotogenic model*, *Phys. Lett. B* **860** (2025) 139171 [[2409.12547](#)].
- [56] T. Nomura and H. Okada, *Zee model in a non-holomorphic modular A_4 symmetry*, *Phys. Lett. B* **867** (2025) 139618 [[2412.18095](#)].

- [57] T. Nomura, H. Okada and X.-Y. Wang, *A radiative neutrino mass model with leptoquarks under non-holomorphic modular A_4 symmetry*, *JHEP* **09** (2025) 163 [[2504.21404](#)].
- [58] T. Nomura and H. Okada, *Neutrino mass model at a three-loop level from a non-holomorphic modular A_4 symmetry*, [2506.02639](#).
- [59] T. Nomura and H. Okada, *A new type of lepton seesaw model in a modular A_4 symmetry*, [2503.19251](#).
- [60] S.K. Kang and H. Okada, *Neutrino masses and mixing in an axion model*, *Eur. Phys. J. C* **85** (2025) 917 [[2408.14942](#)].
- [61] G.-J. Ding, J.-N. Lu, S.T. Petcov and B.-Y. Qu, *Non-holomorphic modular S_4 lepton flavour models*, *JHEP* **01** (2025) 191 [[2408.15988](#)].
- [62] C.-C. Li, J.-N. Lu and G.-J. Ding, *Non-holomorphic modular A_5 symmetry for lepton masses and mixing*, *JHEP* **12** (2024) 189 [[2410.24103](#)].
- [63] H. Okada and Y. Orikasa, *A radiative seesaw in a non-holomorphic modular S_3 flavor symmetry*, [2501.15748](#).
- [64] T. Kobayashi, H. Okada and Y. Orikasa, *Zee-Babu model in a non-holomorphic modular A_4 symmetry and modular stabilization*, [2502.12662](#).
- [65] M.A. Loualidi, M. Miskaoui and S. Nasri, *Nonholomorphic A_4 modular invariance for fermion masses and mixing in $SU(5)$ GUT*, *Phys. Rev. D* **112** (2025) 015008 [[2503.12594](#)].
- [66] X. Zhang and Y. Reyimuaji, *Inverse seesaw model in nonholomorphic modular A_4 flavor symmetry*, *Phys. Rev. D* **112** (2025) 075050 [[2507.06945](#)].
- [67] T. Nomura and H. Okada, *Lepton seesaw model in a modular A_4 symmetry*, [2409.10912](#).
- [68] M. Abbas, *Lepton Masses and Mixing in Nonholomorphic Modular A_4 Symmetry*, *PHEP* **2025** (2025) 7.
- [69] C.-C. Li and G.-J. Ding, *Lepton models from non-holomorphic A'_5 modular flavor symmetry*, [2509.15183](#).
- [70] M. Dey, *The Seesaw Evaded Modular Dirac Framework*, [2509.10373](#).
- [71] S.K. Nanda, M. Ricky Devi and S. Patra, *Non-Holomorphic A_4 Modular Symmetry in Type-I Seesaw: Implications for Neutrino Masses and Leptogenesis*, [2509.22108](#).
- [72] B. Kumar and M.K. Das, *Leptogenesis, $0\nu\beta\beta$ and lepton flavor violation in modular left-right asymmetric model with polyharmonic Maa β forms*, *JHEP* **09** (2025) 071 [[2504.21701](#)].
- [73] H. Ishimori, T. Kobayashi, H. Ohki, Y. Shimizu, H. Okada and M. Tanimoto, *Non-Abelian Discrete Symmetries in Particle Physics*, *Prog. Theor. Phys. Suppl.* **183** (2010) 1 [[1003.3552](#)].
- [74] G. Chauhan, P.S.B. Dev, I. Dubovyk, B. Dziewit, W. Flieger, K. Grzanka et al., *Phenomenology of lepton masses and mixing with discrete flavor symmetries*, *Prog. Part. Nucl. Phys.* **138** (2024) 104126 [[2310.20681](#)].
- [75] T. Kobayashi, Y. Shimizu, K. Takagi, M. Tanimoto, T.H. Tatsuishi and H. Uchida, *Finite modular subgroups for fermion mass matrices and baryon/lepton number violation*, *Phys. Lett. B* **794** (2019) 114 [[1812.11072](#)].

- [76] H. Okada and Y. Orikasa, *Modular S_3 symmetric radiative seesaw model*, *Phys. Rev. D* **100** (2019) 115037 [[1907.04716](#)].
- [77] S. Mishra, *Neutrino mixing and Leptogenesis with modular S_3 symmetry in the framework of type III seesaw*, [2008.02095](#).
- [78] S.K. Kang, R. Kumar and H. Okada, *Radiative Dirac Neutrino Masses from Modular S_3 Symmetry in an Axion Model*, [2601.22740](#).
- [79] D. Meloni and M. Parriciatu, *A simplest modular S_3 model for leptons*, *JHEP* **09** (2023) 043 [[2306.09028](#)].
- [80] S. Marciano, D. Meloni and M. Parriciatu, *Minimal seesaw and leptogenesis with the smallest modular finite group*, *JHEP* **05** (2024) 020 [[2402.18547](#)].
- [81] M. Belfkir, M.A. Loualidi and S. Nasri, *Fermion Masses and Mixing in Pati–Salam Unification with S_3 Modular Symmetry*, *PTEP* **2025** (2025) 033B05 [[2501.00302](#)].
- [82] T. Nomura, H. Okada and H. Otsuka, *Texture zeros realization in a three-loop radiative neutrino mass model from modular A_4 symmetry*, *Nucl. Phys. B* **1004** (2024) 116579 [[2309.13921](#)].
- [83] M. Ricky Devi, *Neutrino Masses and Higher Degree Siegel Modular Forms*, [2401.16257](#).
- [84] J. Gogoi, L. Sarma and M.K. Das, *Leptogenesis and dark matter in minimal inverse seesaw using A_4 modular symmetry*, *Eur. Phys. J. C* **84** (2024) 689 [[2311.09883](#)].
- [85] G. Pathak, P. Das and M.K. Das, *Neutrino mass genesis in scoto-inverse seesaw with modular A_4* , *Eur. Phys. J. C* **85** (2025) 569 [[2411.13895](#)].
- [86] T. Nomura and H. Okada, *A More Novel Approach of Radiative Linear Seesaw in a Modular A_4 Symmetry*, *PTEP* **2025** (2025) 043B04 [[2410.21843](#)].
- [87] M. Kashav and S. Verma, *Broken Scaling Neutrino Mass Matrix and Leptogenesis based on A_4 Modular invariance*, [2103.07207](#).
- [88] M. Kashav and S. Verma, *On minimal realization of topological Lorentz structures with one-loop seesaw extensions in A_4 modular symmetry*, *JCAP* **03** (2023) 010 [[2205.06545](#)].
- [89] T. Kobayashi, T. Nomura and T. Shimomura, *Type II seesaw models with modular A_4 symmetry*, [1912.00637](#).
- [90] T. Nomura and H. Okada, *Quark and lepton model with flavor specific dark matter and muon $g-2$ in modular A_4 and hidden $U(1)$ symmetries*, *Phys. Dark Univ.* **49** (2025) 101986 [[2304.13361](#)].
- [91] J. Kim and H. Okada, *Fermi-LAT GeV excess and muon $g-2$ in a modular A_4 symmetry*, [2302.09747](#).
- [92] M.R. Devi, *Retrieving texture zeros in 3+1 active-sterile neutrino framework under the action of A_4 modular-invariants*, [2303.04900](#).
- [93] A. Dasgupta, T. Nomura, H. Okada, O. Popov and M. Tanimoto, *Dirac Radiative Neutrino Mass with Modular Symmetry and Leptogenesis*, [2111.06898](#).
- [94] S. Centelles Chuliá, R. Kumar, O. Popov and R. Srivastava, *Neutrino mass sum rules from modular A_4 symmetry*, *Phys. Rev. D* **109** (2024) 035016 [[2308.08981](#)].
- [95] I. de Medeiros Varzielas, M. Levy, J.T. Penedo and S.T. Petcov, *Quarks at the modular S_4 cusp*, *JHEP* **09** (2023) 196 [[2307.14410](#)].

- [96] G.-J. Ding, S.F. King and C.-Y. Yao, *Modular $S_4 \times SU(5)$ GUT*, *Phys. Rev. D* **104** (2021) 055034 [2103.16311].
- [97] S.F. King and Y.-L. Zhou, *Trimaximal TM_1 mixing with two modular S_4 groups*, *Phys. Rev. D* **101** (2020) 015001 [1908.02770].
- [98] I. de Medeiros Varzielas and J. Lourenço, *Two A_5 modular symmetries for Golden Ratio 2 mixing*, *Nucl. Phys. B* **984** (2022) 115974 [2206.14869].
- [99] C.-Y. Yao, X.-G. Liu and G.-J. Ding, *Fermion masses and mixing from the double cover and metaplectic cover of the A_5 modular group*, *Phys. Rev. D* **103** (2021) 095013 [2011.03501].
- [100] X.-G. Liu, C.-Y. Yao, B.-Y. Qu and G.-J. Ding, *Half-integral weight modular forms and application to neutrino mass models*, *Phys. Rev. D* **102** (2020) 115035 [2007.13706].
- [101] P.F. de Salas, D.V. Forero, S. Gariazzo, P. Martínez-Miravé, O. Mena, C.A. Ternes et al., *2020 global reassessment of the neutrino oscillation picture*, *JHEP* **02** (2021) 071 [2006.11237].
- [102] F. Capozzi, E. Di Valentino, E. Lisi, A. Marrone, A. Melchiorri and A. Palazzo, *Unfinished fabric of the three neutrino paradigm*, *Phys. Rev. D* **104** (2021) 083031 [2107.00532].
- [103] I. Esteban, M.C. Gonzalez-Garcia, M. Maltoni, I. Martinez-Soler, J.P. Pinheiro and T. Schwetz, *NuFit-6.0: updated global analysis of three-flavor neutrino oscillations*, *JHEP* **12** (2024) 216 [2410.05380].
- [104] P. Huber, M. Lindner and W. Winter, *Simulation of long-baseline neutrino oscillation experiments with GLOBES (General Long Baseline Experiment Simulator)*, *Comput. Phys. Commun.* **167** (2005) 195 [hep-ph/0407333].
- [105] P. Huber, J. Kopp, M. Lindner, M. Rolinec and W. Winter, *New features in the simulation of neutrino oscillation experiments with GLOBES 3.0: General Long Baseline Experiment Simulator*, *Comput. Phys. Commun.* **177** (2007) 432 [hep-ph/0701187].
- [106] DUNE collaboration, *Experiment Simulation Configurations Approximating DUNE TDR*, 2103.04797.
- [107] DUNE collaboration, *Long-baseline neutrino oscillation physics potential of the DUNE experiment*, *Eur. Phys. J. C* **80** (2020) 978 [2006.16043].
- [108] G.L. Fogli, E. Lisi, A. Marrone, D. Montanino and A. Palazzo, *Getting the most from the statistical analysis of solar neutrino oscillations*, *Phys. Rev. D* **66** (2002) 053010 [hep-ph/0206162].
- [109] P. Huber, M. Lindner and W. Winter, *Superbeams versus neutrino factories*, *Nucl. Phys. B* **645** (2002) 3 [hep-ph/0204352].
- [110] A. Baur, *FlavorPy*, 2024. 10.5281/zenodo.11060597.
- [111] KATRIN collaboration, *Direct neutrino-mass measurement based on 259 days of KATRIN data*, *Science* **388** (2025) adq9592 [2406.13516].
- [112] PROJECT 8 collaboration, *The Project 8 Neutrino Mass Experiment*, in *Snowmass 2021*, 3, 2022 [2203.07349].
- [113] APPEC COMMITTEE collaboration, *Double Beta Decay APPEC Committee Report*, 1910.04688.
- [114] GERDA collaboration, *Probing Majorana neutrinos with double- β decay*, *Science* **365** (2019) 1445 [1909.02726].

- [115] CUORE collaboration, *First Results from CUORE: A Search for Lepton Number Violation via $0\nu\beta\beta$ Decay of ^{130}Te* , *Phys. Rev. Lett.* **120** (2018) 132501 [[1710.07988](#)].
- [116] KAMLAND-ZEN collaboration, *Search for Majorana Neutrinos with the Complete KamLAND-Zen Dataset*, [2406.11438](#).
- [117] LEGEND collaboration, *The Large Enriched Germanium Experiment for Neutrinoless $\beta\beta$ Decay: LEGEND-1000 Preconceptual Design Report*, [2107.11462](#).
- [118] NEXO collaboration, *nEXO: neutrinoless double beta decay search beyond 10^{28} year half-life sensitivity*, *J. Phys. G* **49** (2022) 015104 [[2106.16243](#)].
- [119] PLANCK collaboration, *Planck 2018 results. VI. Cosmological parameters*, *Astron. Astrophys.* **641** (2020) A6 [[1807.06209](#)].
- [120] DESI collaboration, *DESI 2024 VI: cosmological constraints from the measurements of baryon acoustic oscillations*, *JCAP* **02** (2025) 021 [[2404.03002](#)].
- [121] EUCLID collaboration, *Euclid preparation - LIV. Sensitivity to neutrino parameters*, *Astron. Astrophys.* **693** (2025) A58 [[2405.06047](#)].
- [122] J.H. Gallier, *The schur complement and symmetric positive semidefinite (and definite) matrices*, Tech. Rep. <https://www.cis.upenn.edu/~jean/schur-comp.pdf>, University of Pennsylvania (2010).